Research and Development of Low-Power DC Anode-Radiation-Cooled Arcjet Thrusters Using Low-Toxicity Propellants

IEPC-2017-150

Presented at the 35th International Electric Propulsion Conference
Georgia Institute of Technology • Atlanta, Georgia • USA
October 8 – 12, 2017

Katsuya Shimogaito[1], Suguru Shiraki[2], Yuki Fukutome[3], Kazuyoshi Okuda[4],
Takefumi Mimura[5], Hirokazu Tahara[6], Kyoko Takada[7],
Osaka Institute of Technology,
5-16-1, Omiya, Asahi-ku, Osaka 535-8585, Japan

Ai Momozawa[8]
Tokyo City University,
1-28-1, Tamazutsumi, Setagaya-ku, Tokyo 158-8557, Japan

Daisuke Nakata[9]
Muroran Institute of Technology,
27-1, Mizumoto-Cho, Muroran, Hokkaido 050-8585, Japan

and

Yuichiro Nogawa[10]
Splije,
1-8-2-903, Takezono, Tsukuba, Ibaraki 305-0032, Japan

---

[1] Graduate Student, Major in Mechanical Engineering, Graduate School of Engineering, and hirokazu.tahara@oit.ac.jp.
[2] Graduate Student, Major in Mechanical Engineering, Graduate School of Engineering, and hirokazu.tahara@oit.ac.jp
[3] Graduate Student, Major in Mechanical Engineering, Graduate School of Engineering, and hirokazu.tahara@oit.ac.jp
[4] Graduate Student, Major in Mechanical Engineering, Graduate School of Engineering, and hirokazu.tahara@oit.ac.jp
[5] Graduate Student, Major in Mechanical Engineering, Graduate School of Engineering, and hirokazu.tahara@oit.ac.jp
[6] Professor, Department of Mechanical Engineering, Faculty of Engineering, and hirokazu.tahara@oit.ac.jp
[7] Associate Professor, Department of Intellectual Property, Faculty of Intellectual Property, and kyoko.takada@oit.ac.jp
[8] Assistant Professor, Department of Medical Engineering, Faculty of Engineering, and momozawa@al.t.u-tokyo.ac.jp
[9] Associate Professor, Department of Creativity, Faculty of Aerospace engineering, and nakata@mmm.muroran-it.ac.jp
[10] CEO and Researcher, Electric Propulsion R&D section, and nogawa.yuichiro@gmail.com

Abstract: **The DC arcjet thruster is one of electric propulsion for satellite attitude control and orbital control. Hydrazine is used for an arcjet thruster as the propellant because it can be used together with chemical propulsions. However, hydrazine is high in toxicity, and that is difficult in handling. Therefore, arcjet thrusters using low-toxicity propellants have been investigated all over the world. In this study, 1-3kW class low-power DC water-cooled arcjet thrusters were operated by using Hydroxyl Ammonium Nitrate (HAN: NH_3OHNO_3) series. The target of investigation is to improve thrust performances using HAN (SHP163 decomposed gas). Thrust performances were measured using SHP163 decomposed gas. The results of a thrust of 84 mN, a specific impulse of 215 s, a thrust efficiency of 6.5% were obtained with 1.0 kW. As a comparison, thrust performances were measured using hydrazine decomposed gas. The result of a thrust of 114 mN, a specific impulse of 291 s, a thrust efficiency of 6.2% with 1.1 kW. From these results, the performance with hydrazine decomposed gas is higher than that with SHP163 decomposed gas. Furthermore, we obtained basic characteristics with 1-3kW class low-power DC anode-radiation-cooled arcjet thrusters using nitrogen. And we compared the performances between the anode-radiation-cooled and the water-cooled arcjet thrusters. As a result, all performances of the anode-radiation-cooled arcjet thruster were higher than those of the water-cooled arcjet thruster.**

I. Introduction

In recent years, asteroid exploration, moon, Mars exploration, etc. are actively conducted all over the world as a national project, and electric propulsion is attracting attention as propulsion devices of the aircraft. Arcjet thrusters are a kind of electric propulsion devices, the structure is simpler than other electric propulsion devices, the range of types of propellant that can be used is wide, and the use of a propellant with the chemical propulsion, that is, has the advantage that it is possible to share cylinders for propellants. For that reason, it has been used for orbital control and attitude control of artificial satellites. However, hydrazine (N_2H_4), which has been mainly used as a propellant, can be used in combination with a stable injection and a propellant with a chemical propellant, but it has high deniability and carcinogenicity, is high in handling it takes cost and time. Therefore, the development of a low-toxicity propellant to replace hydrazine is a problem. At Osaka Institute of Technology, HAN series, which is a low-toxicity propellant, is focused on research. Like hydrazine, HAN propellant can be used in combination with chemical propulsion equipment, and additionally has combustion performance beyond hydrazine. Therefore, it is considered to be the center of the next generation satellite propulsion system. In this study, performance comparison HAN propellant and hydrazine was performed using water-cooled arcjet thruster. After through some gas decomposition generators, HAN(SHP163) decomposed gas and hydrazine decomposed gas, which is one kind of HAN decomposed gas, were used.

II. Experimental Equipment

2.1. Schematic diagram of the Experimental Equipment

The experimental equipment is composed of arcjet thruster, propellant supply system, DC power supply system, thrust measurement system, vacuum exhaust system and gas generator. The schematic diagram of the experimental equipment is shown in Figure 1.

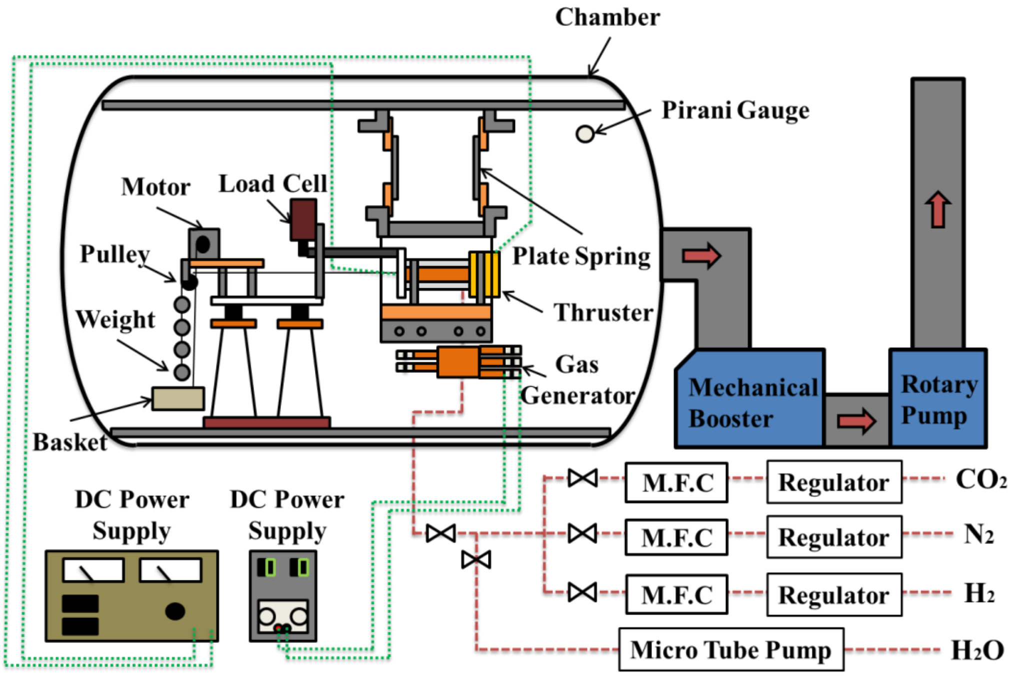

Figure 1. Schematic diagram of the experimental equipment.

2.2. Arcjet Thruster
2.2.1. Water-Cooled Arcjet Thruster

The photo and the cross-sectional view of the water-cooled arcjet thruster are shown in Figure 2. The anode is made of excellent antiseptic SUS304 because we use corrosive HAN. The body is made of polycarbonate. The cathode is made of tungsten because tungsten is high melting point metal. Electrode gap was adjusted by cathode holder. Both the cathode holder and the anode holder are water-cooled for preventing the electrodes from melting down by the operation.

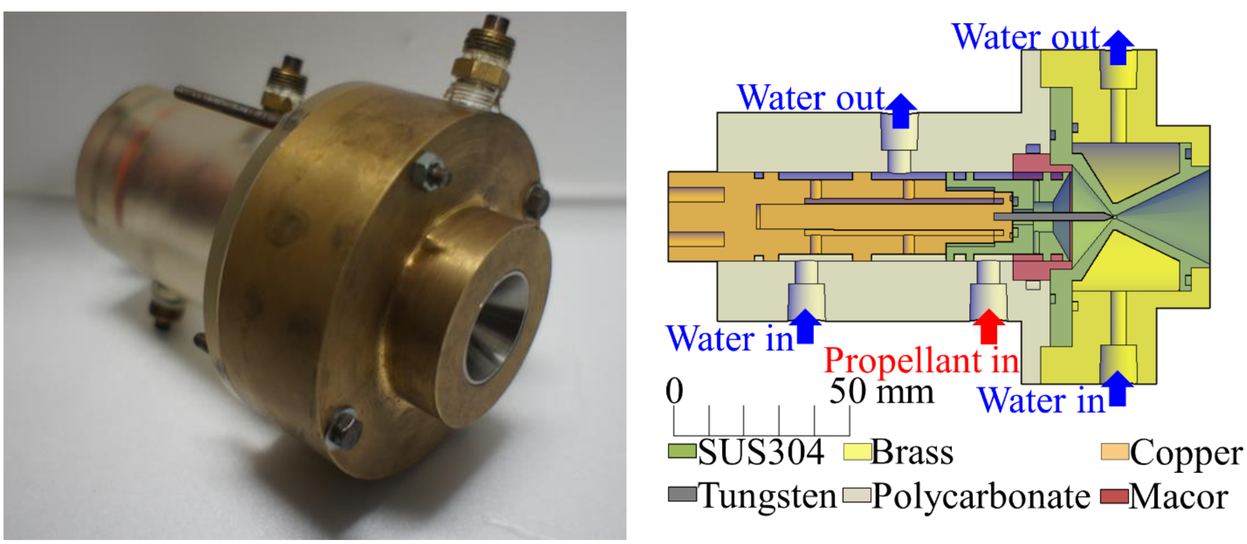

(a) Photo. (b) Cross-Sectional view.
Figure 2. Water-Cooled arcjet thruster.

The schematic and the dimension of electrode configuration are shown in Figure 3 and Table 1 respectively. In this study, electrode gap is 0 mm.

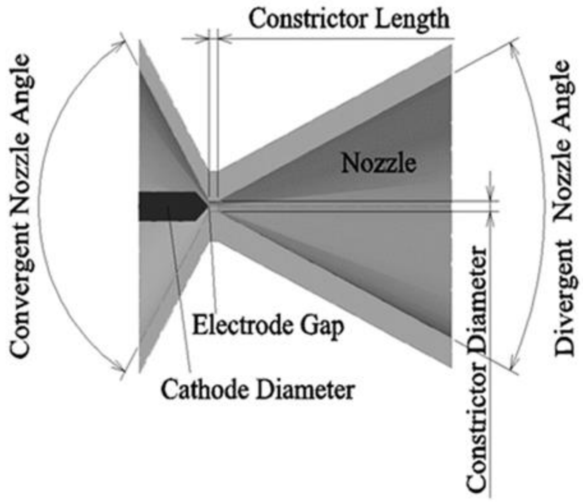

Figure 3. Electrode configuration.

Table 1. Experimental conditions of electrode configuration.

Convergent Nozzle Angle, deg		102
Divergent Nozzle Angle, deg		52
Constrictor	Diameter, mm	1.0
	Length, mm	1.0
Cathode Diameter, mm		2.0 or 3.0

2.2.2. Prototype anode-radiation-cooled arcjet thruster

We developed the prototype anode-radiation-cooled arcjet thruster to improve the performance characteristics. The photo and the cross-sectional view of the prototype anode-radiation-cooled arcjet thruster are shown in Figures 6 and 7. The thruster has a water-cooled cathode holder, and an anode that is radiation-cooled. The anode is made of carbon, which is a high melting point material. The body is made of PBT (Poly butylene terephthalate). The thruster has two propellant supply ports of gas and liquid propellants. The ports are electrically insulated by a ceramics insulator. Propellants are directly injected to the arcjet plenum room. The electrode configuration are the same to the water-cooled arcjet as shown in Table 1 except for the cathode diameter. The cathode diameter of prototype anode-radiation-cooled arcjet thruster is 3.0 mm.

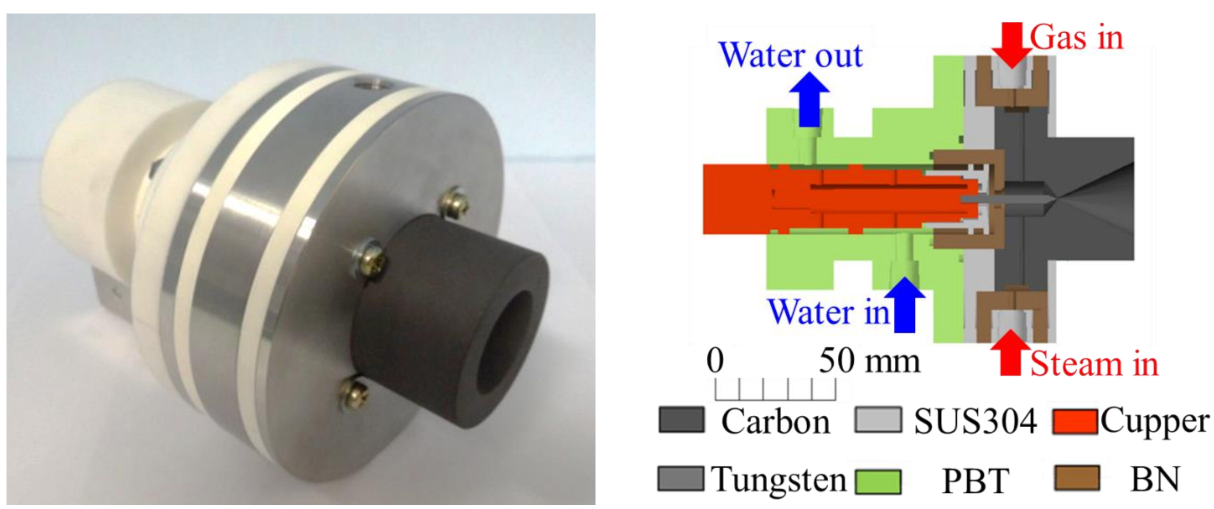

(a) Photon-cooled arcjet. (b) Cross-Sectional view.

Figure 4. Prototype anode-radiation-cooled arcjet thruster.

2.3. Propellant Supply System

In this study, nitrogen, SHP163 decomposed gas and hydrazine decomposed gas were used as propellants. Nitrogen (N_2), hydrogen (H_2), carbon dioxide (CO_2) are supplied through the regulator and then adjusted to the designated flow rate set by the mass flow controller (KOFLOC, Model3600 series). The accuracy of the mass flow controller is ±1.0%. In addition, the temperature shift is ±1.0 K. The micro tube pump (Tokyo Rikakikai Co. Ltd., MP1000-A) is used for water (H_2O) supply. The micro tube pump can adjust the flow rate within the range of 10-180 ml/h, the flow accuracy is ± 2%, and the discharge pressure is 147 kPa.

2.4. Vacuum exhaust system

The photos of the vacuum chamber and the vacuum pumps are shown in Figures 5 and 6. The vacuum chamber used in this study is cylindrical and made of stainless steel. The inner diameter of the vacuum chamber is 1.2 m, and the length is 2 m. A rotary pump (Osaka Vacuum Equipment Manufactory, exhaust speed 600 m^3/h) and a mechanical booster (Osaka Vacuum Equipment Manufactory, exhaust speed 600 m3/h) are used to have a vacuum condition of 5 Pa.

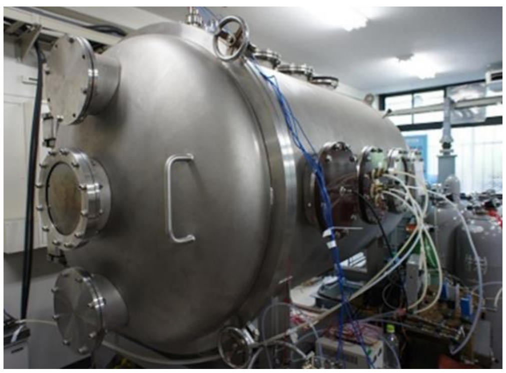

Figure 5. Photo of the vacuum chamber.

Figure 6. Photo of the vacuum pump.

2.5. Thrust Measurement System

In this experiment with water-cooled arcjet, a thrust measurement system with plate springs as shown in Figure 7 and Figure 8 was used. Plate springs are made of stainless steel ones with 90 mm in length, 20 mm in width and 0.4 mm in thickness. The arcjet thruster was mounted below the plate spring. The load cell (Agent A & D Co., Ltd., U2X1-0.5LA) is settled on the same axis as the central axis of the thruster. The load cell is pushed by thrust. Calibration was taken by pulling the thruster with weights in the axial direction. We obtained a linear relationship between the applied weight and the output of the amplifier. Figure 9 shows a typical calibration data. It is very linear line. In addition, a heat shield was mounted near the thrust measurement system in order to prevent the plate spring from being heated. The heat shield is made of copper.

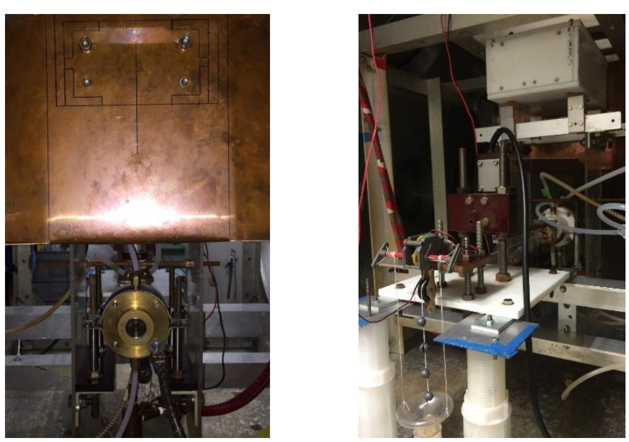

Figure 7. Photo of the thrust measurement system.

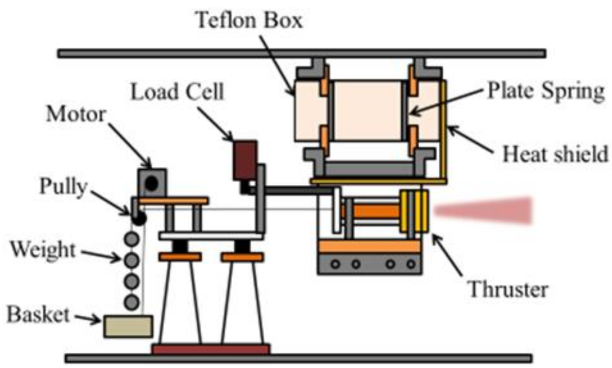

Figure 8. Shematic view of
thrust measurement system.

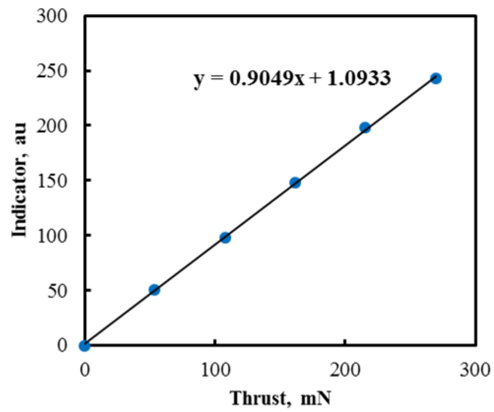

Figure 9. Typical calibration line.

2.6. Gas Generator

In this experiment SHP163 decomposed gas which is one kind of HAN propellant is used. The gas generator was installed to vaporize water, which is one of combustible components of SHP163 decomposed gas. Five glow plugs are used for the heat source of the gas generator. The tip part is a heating element, and when power is applied, the tip element rises to about 1,100 °C. And glows red. Water is brought into contact with this red heat part, and direct heating is performed to vaporize. Also, copper was used for the body with excellent thermal conductivity, so that the interior of the body was heated. A photograph of the gas generator is shown in Figure 10, and a photograph of the glow plug is shown in Figure 11.

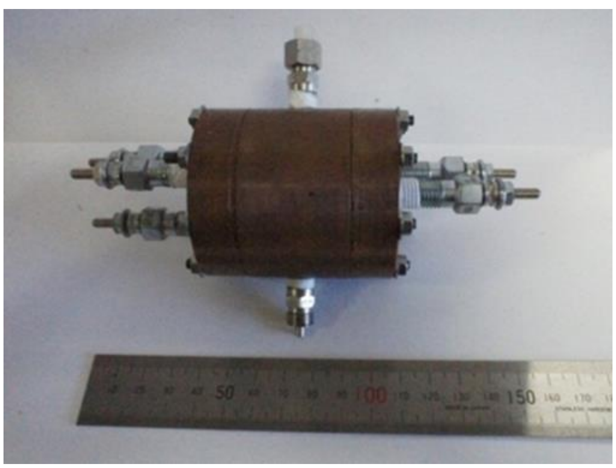

Figure 10. Gas generator.

Figure 11. Metal glow plug.

2.7. Thermal measurement system

A thermocouple (Chinook sheath thermocouple 1 HKF 011, Inc.) was used for checking the operating state and temperature condition of the arc jet thruster. The thermocouple used is K type, and measurement temperature range is -200 □ to 1050 □. Considering the attachment to the thruster, the length of the sheath is set to 100 mm and the outer diameter is set to 1 mm. A photograph of a thermocouple is shown in Figure 12. The detected temperature is input as an electric signal to a personal computer via a data logger (LR 8402 manufactured by HIOKI EK CO., LTD.).

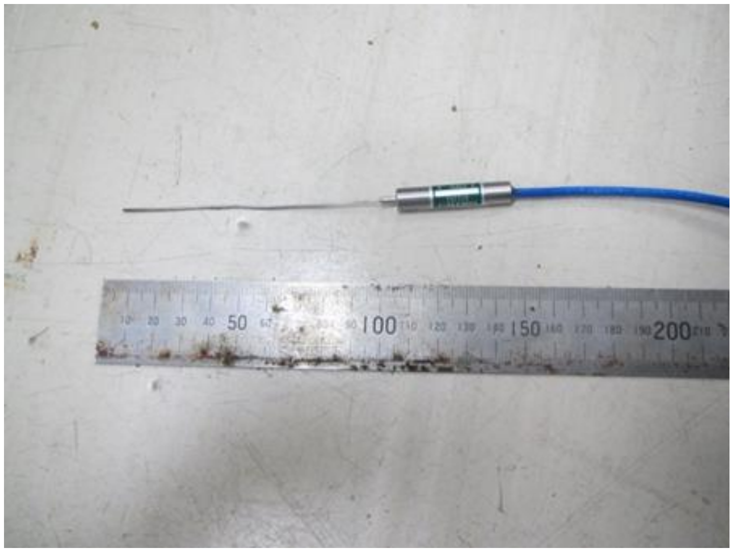

Figure 12. Thermocouple.

III. Performance comparison with HAN (SHP163 decomposed gas) and hydrazine decomposed gases

3.1. Experimental conditions

We measured the performance of HAN (SHP163 decomposed gas) and compared with that of hydrazine decomposed gas using water-cooled arcjet thruster. Experimental conditions in performance comparison are shown in Table 2.

Table 2. Experimental conditions for performance comparison with SHP163 decomposed gas and hydrazine decomposed gas.

Propellant	SHP163 decomposed gas	Hydrazine decomposed gas
Mass Flow Rate, mg/s	40, 50, 60	
Current, A	7.0, 8.0, 9.0, 10.0	
Cathode Diameter, mm	2.0	

3.2. Experimental result

Water-Cooled arcjet plasma plumes are shown in Figure 13 and the results of performance comparison of SHP163 and hydrazine decomposed gases are shown in Figure 14.

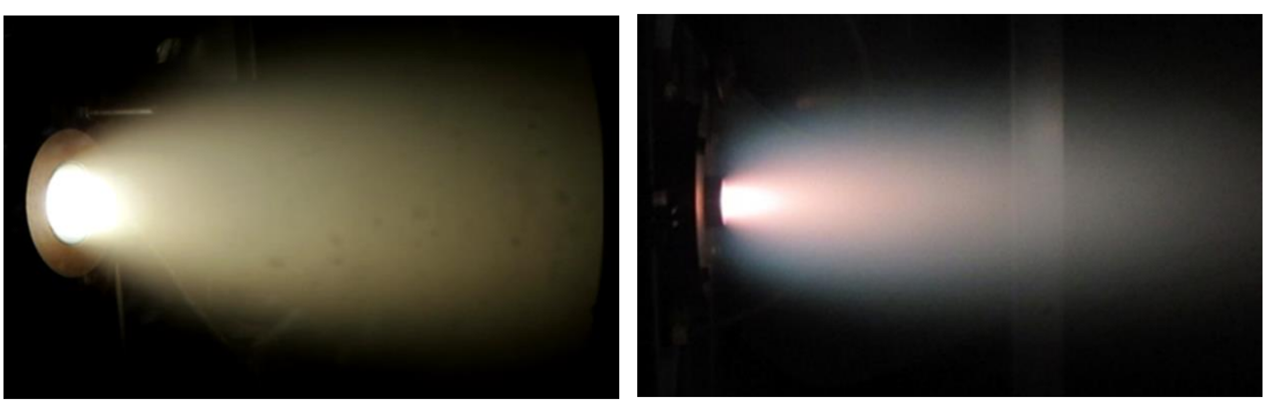

(a) HAN (SHP163 decomposed gas). (b) Hydrazine decomposed gas.

Figure 13. Photo of water-cooled arcjet plasma plumes.

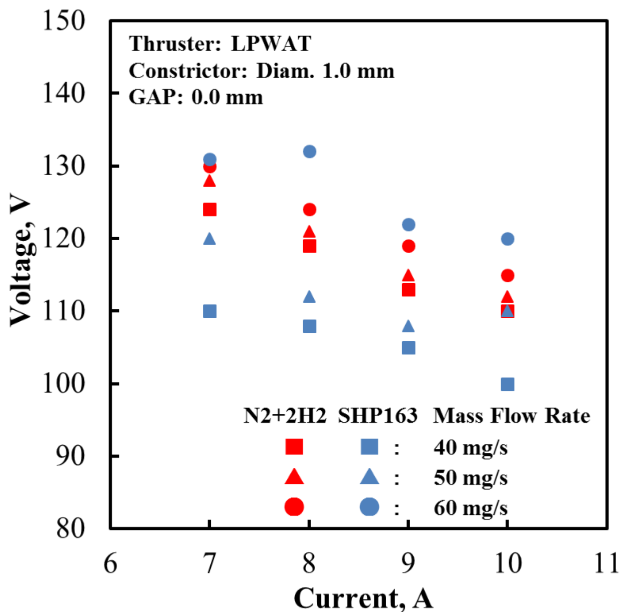

(a) Discharge voltage vs. current.

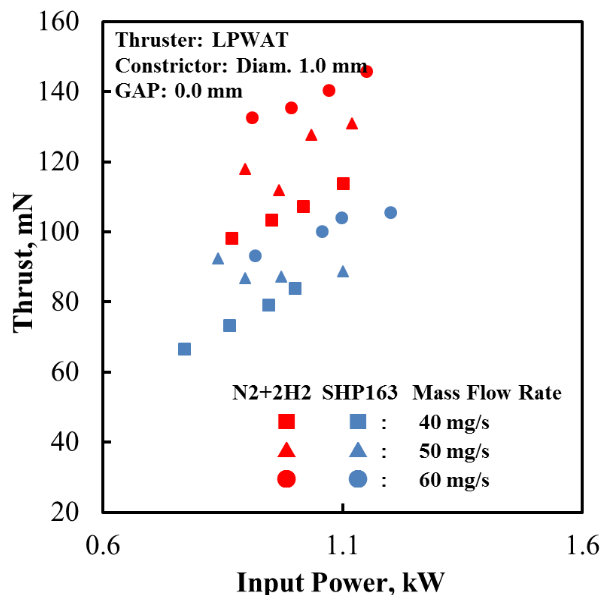

(b) Thrust vs. input power.

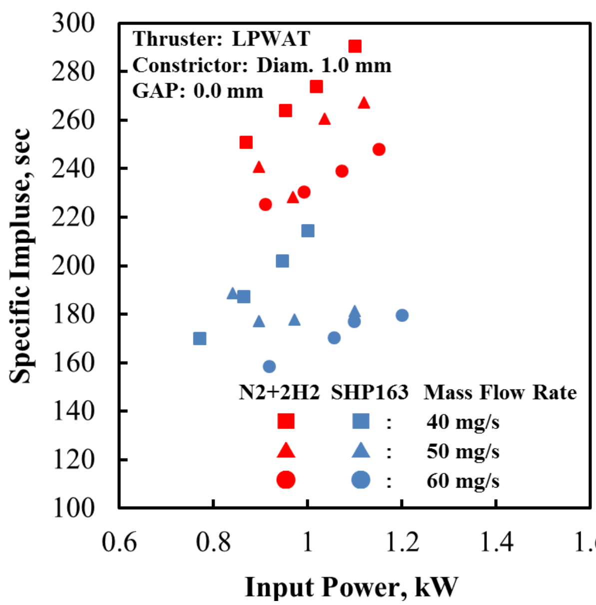

(c) Specific impulse vs. input power.

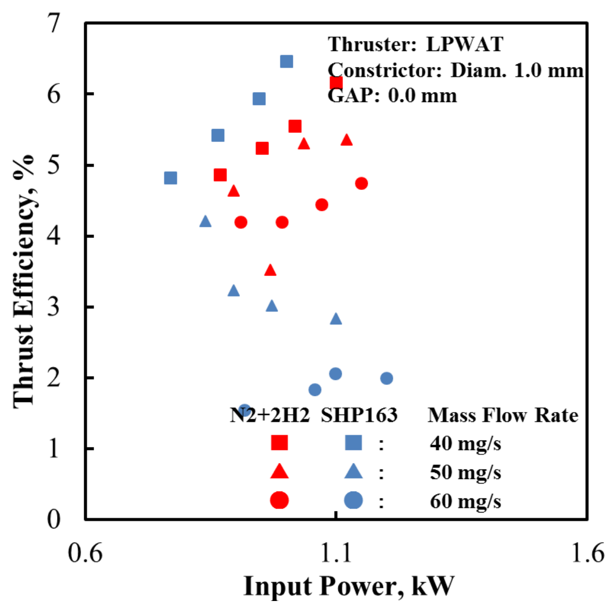

(d) Thrust efficiency vs. input power.

Figure 14. Performance comparison of SHP163 decomposed gas and hydrazine decomposed gas.

As shown in Figure 13, we could confirm stable operation using SHP163 decomposed gas. As shown in Figure 14, thrusts with SHP163 and hydrazine decomposed gases are 106 mN and 146 mN, respectively, with specific impulses of 215 s and 338 s at input powers of 1.36 kW and 1.33 kW, and thrust efficiencies are 6.5% and 6.2%, respectively. As a result, thrust performances of SHP163 decomposed gas is lower than that of hydrazine decomposed gas. In addition, we found severe cathode erosion after the operation using SHP163 decomposed gas. The photo of the cathode after the experiments is shown in Figure 15. The severe cathode erosion reduces the internal volume of the plenum room. Therefore, the plenum pressure decreased. I think the performance of thrust worsened by that. Also, there is a possibility that gaseous water in SHP163 decomposed gas is cooled by water cooling of the anode part and returned to liquid. I think that the thrust performance may have deteriorated even by that. Therefore, we consider solving the problem by changing the anode part to the anode radiation cooling type instead of water cooling.

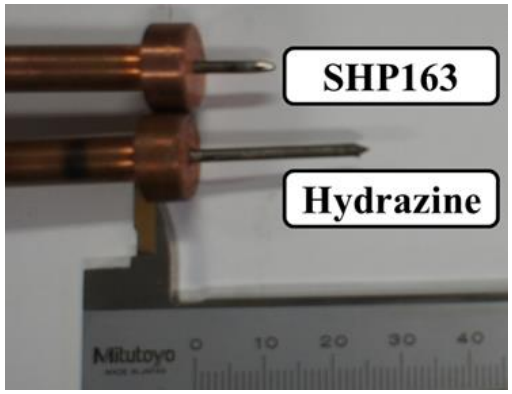

Figure 15. Photo of cathode after experiments.

IV. Performance comparison with water-cooled arcjet thruster and prototype anode-radiation-cooled arcjet thruster

4.1. Experimental conditions

We measured the basic performance of the prototype anode-radiation-cooled arcjet thruster and compared with that of the water-cooled arcjet thruster. As the propellant, nitrogen was used because it is easy for initial ignition and stable operation. Experimental conditions are shown in Table 3.

Table 3. Experimental conditions for performance with prototype anode-radiation-cooled arcjet thruster.

Propellant	Nitrogen
Flow Rate, mg/s	30
Current, A	15
Cathode Diameter, mm	3.0

4.2. Experimental result

The photo of the prototype anode-radiation-cooled arcjet plasma plumes are shown in Figure 16, and the results of performance are shown in Figure 17. As shown in Figure 17, thrust of the prototype anode-radiation-cooled arcjet thruster and the water-cooled arcjet thruster are 83 mN and 80 mN, respectively, with specific impulses of 283 s and 273 s at input powers of 0.705 kW and 0.66 kW, and thrust efficiencies are 10.8% and 8.6%, respectively. As a result, thrust performances of the prototype anode-radiation-cooled arcjet thruster are higher than that of the water-cooled arcjet thruster. The thermal energy loss by water cooling at the anode was reduced.

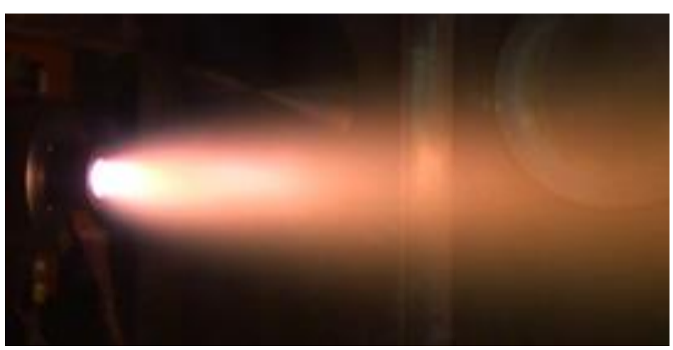
Figure 16. Photo of plasma plume of prototype anode-radiation-cooled arcjet thruster.

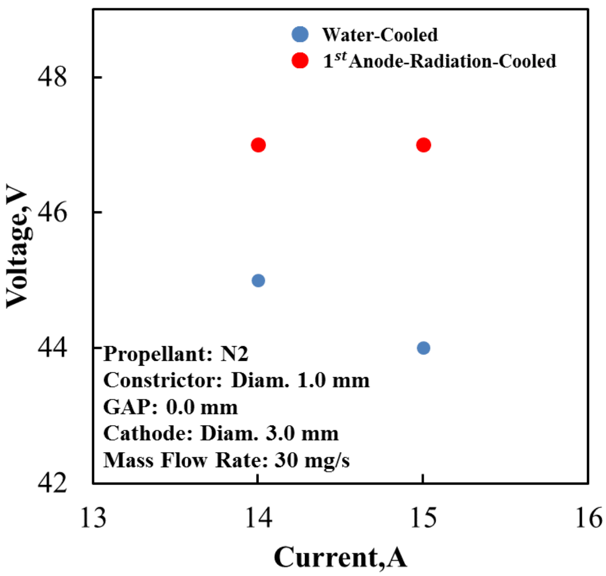

(a) Discharge voltage vs. current.

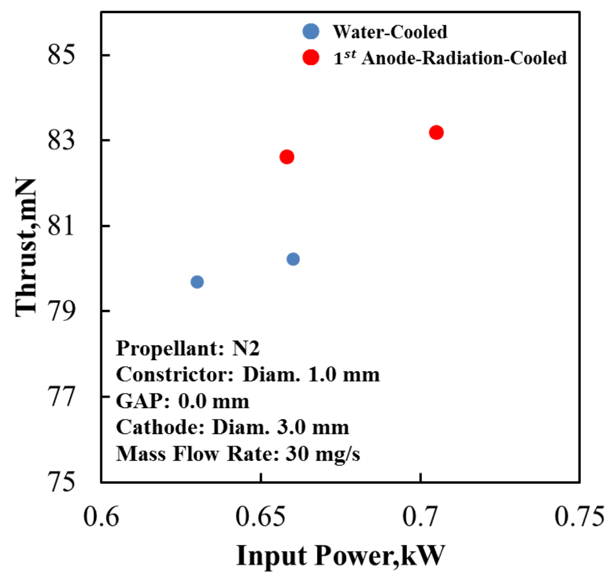

(b) Thrust vs. input power.

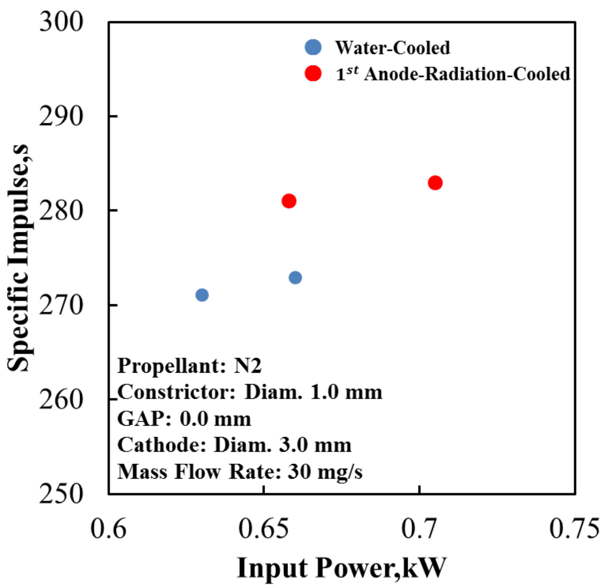

(c) Specific impulse vs. input power.

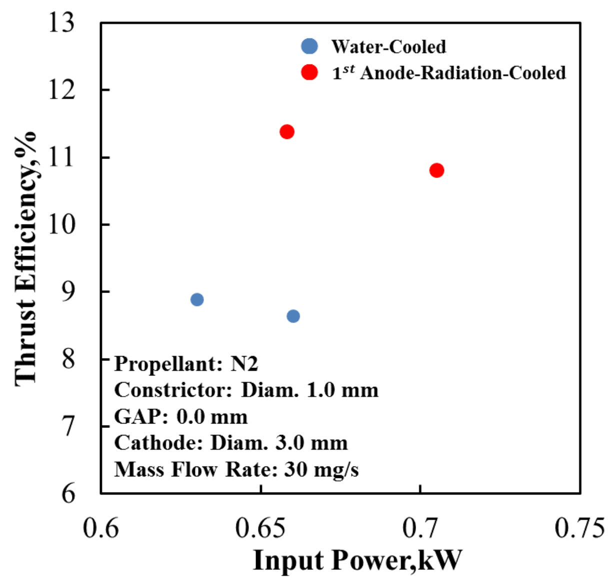

(d) Thrust efficiency vs. input power.

Figure 17. Performance comparison of prototype anode-radiation-cooled arcjet thruster and water-cooled arcjet thruster.

V. Development of improved type anode-radiation-cooled arcjet thruster using thermal analysis

At the prototype anode-radiation-cooled arcjet thruster used in the previous section, the insulator is pressed by the SUS304 anode holder. The insulator was broken by expansion of the anode holder during long time operation. Therefore, we developed improved type anode-radiation-cooled arcjet thruster. The above problem is solved by attaching an insulator to the exterior of the thruster. The conditions of electrode configuration are the same as those of the water-cooled arcjet shown in Table 1 except for the cathode diameter. The cathode diameter of improved type anode-radiation-cooled arcjet thruster is 3.0 mm.

5.1. Thermal analysis condition

FEM analysis to know the temperature distribution was performed by Thermal Desktop (Cullimore and Ring Technologies, Inc). Analysis model of the improved type anode-radiation-cooled arcjet thruster is shown in Figure 18, cross-sectional view of the improved type anode-radiation-cooled arcjet thruster is shown in Figure 19, and the schematic view of the heat transfer coefficient definition points are shown in Figure 20. Also, analysis conditions are shown in Table 4. In this study water cooled condition defines temperature of the water attachment area as 293.15 K. The heat load is applied on the cathode tip was defined to 12.0% of total input power. And the heat load to the anode inner surface tip was defined to 26.8% of total input power. These values are calculated from the energy balance obtained from the temperature measurement experiment with the prototype anode-radiation-cooled arcjet thruster. And the value of the input power is used.

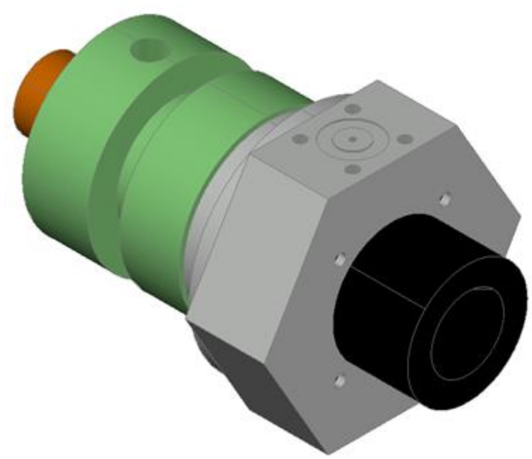

Figure 18. Analysis model of improved type anode-radiation-cooled arcjet thruster.

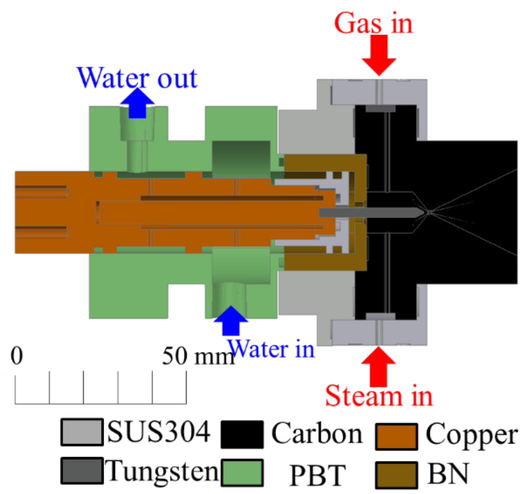

Figure 19. Cross-sectional view of improved type anode-radiation-cooled arcjet thruster.

The contact conditions shown in Table 4 were obtained by calculating the heat transfer coefficient to the position shown in Figure 20. Approximate values of the heat transfer resistance value were calculated using equation (1), and the reciprocal thereof was taken as the heat transfer coefficient.

$$R = \frac{1}{\frac{1}{\frac{Z_1}{\lambda_1} + \frac{1}{h_0} + \frac{Z_2}{\lambda_2}} \cdot \frac{P}{H} + \frac{\lambda_f}{Z_1 + Z_2}\left(1 - \frac{P}{H}\right)} \quad (1)$$

$$\frac{1}{h_0} = 2.3 \text{ x } 10^{-5}\left(\frac{1}{\lambda_1} + \frac{1}{\lambda_2}\right) \quad (2)$$

R = heat transfer resistance value
Z = solid contact surface roughness (maximum roughness)
H = hardness
P = pressing pressure of solid surface
λ = thermal conductivity

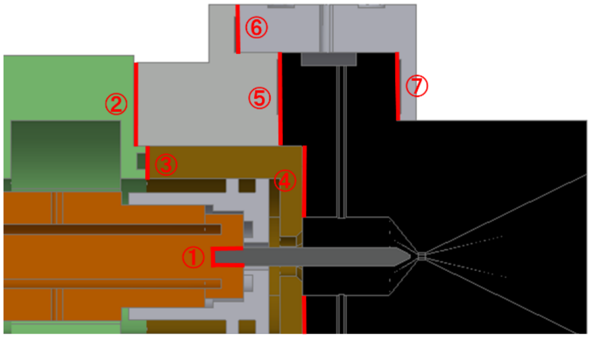

Figure 20. Schematic view of heat transfer coefficient definition points.

Table 4. Analysis conditions for Performance with improved type anode-radiation-cooled arcjet thruster.

Input power, W	Total	1000
	Cathode	120
	Anode	268
Temperature of water-cooled, K		293.15
Number of mesh	Total	143358
	Cathode	4323
	Anode	34228
Heat transfer coefficient, W/m^2K	1	100000
	2	80
	3	2082
	4	84278
	5	3450
	6	3075
	7	4401

5.2. Thermal analysis result

The temperature distribution of the improved type anode-radiation-cooled arcjet thruster is shown in Figures 21 and 25. As shown in Figure 21, all component temperature of the improved type anode-radiation-cooled arcjet thruster was confirmed lower than the melting point. As shown in Figure 22, a maximum temperature of about 3286 K was obtained at the cathode tip. The temperature was lower than the melting point of tungsten. As all results of thermal analysis, thermal design of the thruster was acceptable.

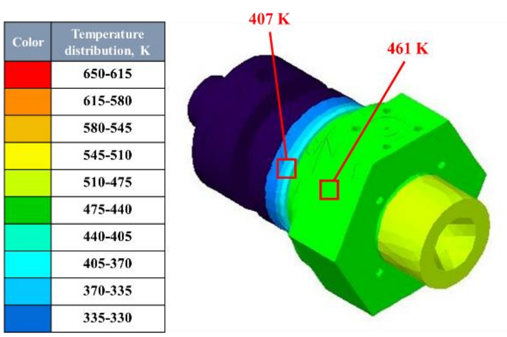

Figure 21. Analysis result of entire thruster.

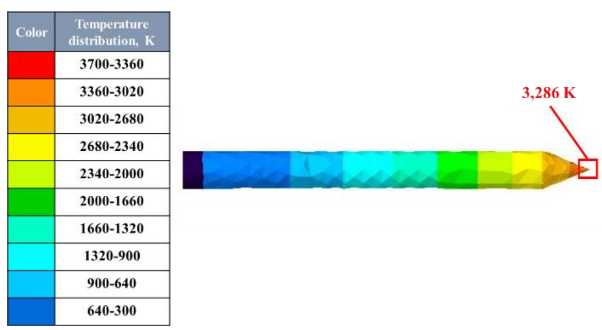

Figure 22. Analysis result of cathode.

5.3. Development of improve type anode-radiation-cooled arcjet thruster

The photo of the improved type anode-radiation-cooled arcjet thruster is shown in Figure 23.

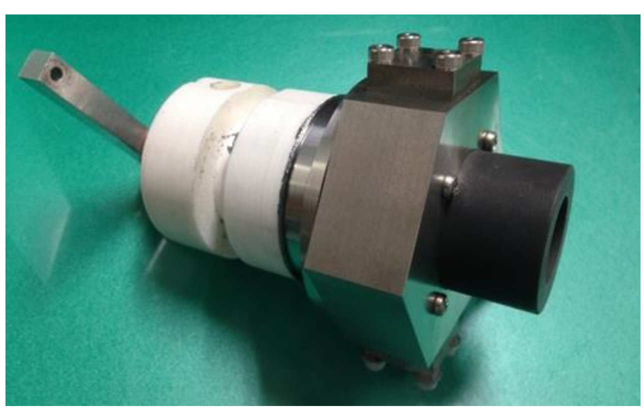

Figure 23. Photo of the improved type anode-radiation-cooled arcjet thruster.

VI. Temperature measurement experiment and comparison with calculated temperature distribution

Temperature measurement was carried out to achieve consistency of the calculated temperature distribution. A sheath thermocouple K type was used for temperature measurement. The operating conditions are shown in Table 5. The temperature measurement position is shown in Figure 24.

Table 5. Experiment conditions.

Cathode Diameter, mm	3.0
Mass Flow Rate, mg/s	60
Current, A	16
Voltage, V	43
Input Power, W	688

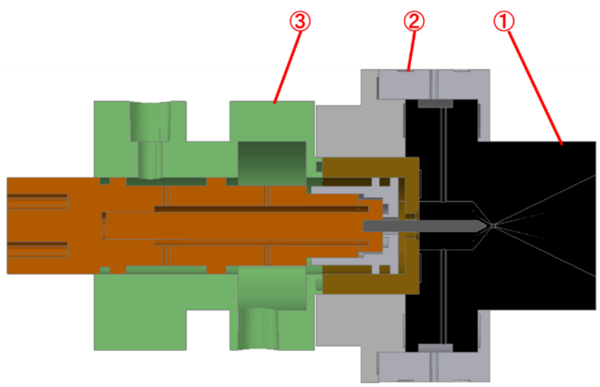

Figure 24. Measurement position in temperature measurement experiment.

6.2. Experimental result

The result of the temperature measurement experiment is shown in Figure 25. The temperature of the anode approaches a constant value of 430 K. Also, the temperature of the body approaches a constant value of 330 K. In this experiment, it was confirmed that the thruster has no thermal problem in the thermal design of improved type anode-radiation-cooled arcjet thruster. In order to compare the current temperature measurement result with the calculated temperature distribution, the input power in the analysis was set to 688 W which is the input power in the experiment, and the analysis calculation time was set to 3600 s which is the current operation time. The input power are shown in Table 6. The calculated temperature distribution is shown in Figure 26.

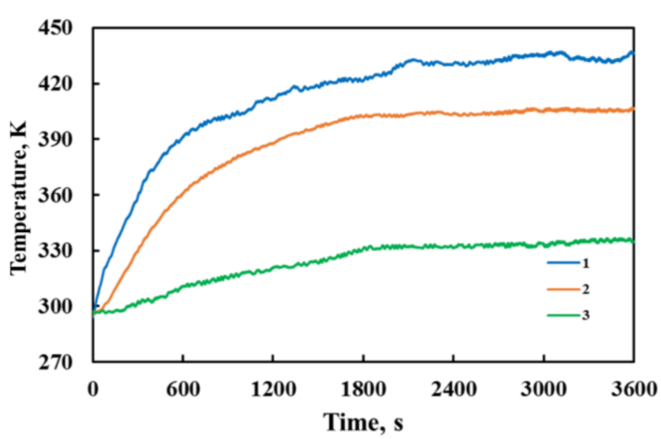

Figure 25. Temperature measurement result.

Table 6. Input power.

	Energy Ratio,%	Input Power, W
Total	100	688
Cathode	12.0	82.6
Anode	26.8	184.4

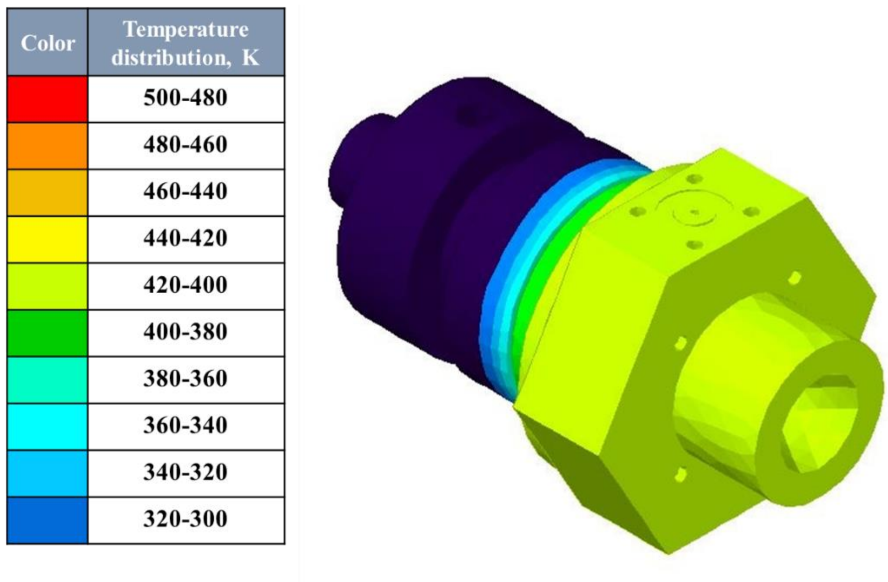

Figure 26. Calculated temperature distribution for comparison with temperature measurement result.

The temperature comparison of the anode is shown in Figure 27. From Figure 27, the maximum error was less than 20 K. A similar tendency was confirmed from the temperature measurement result and the calculated temperature distribution from Figure 27.

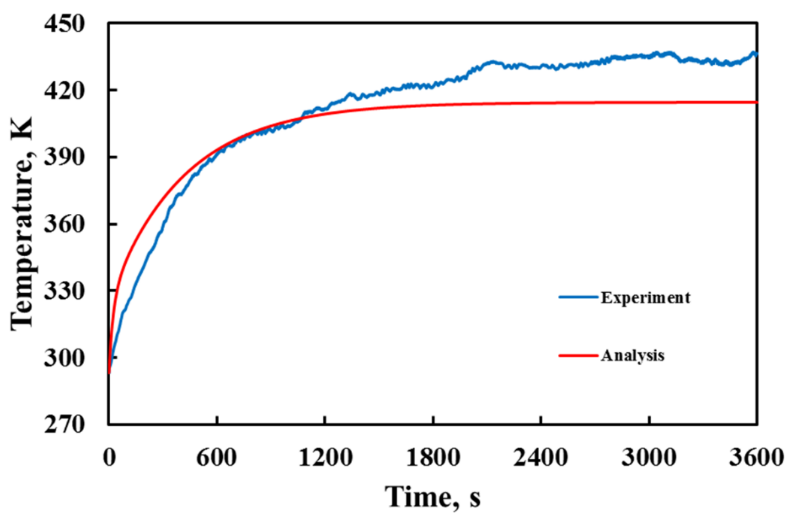

Figure 27. Comparison of temperature by analysis and experiment (anode).

VII. Conclusion

7.1. Performance comparison with HAN (SHP163 decomposed gas) and hydrazine decomposed gas

We confirmed stable operation of arcjet using SHP163 decomposed gas. However, thrust performances of SHP163 decomposed gas was lower than that of hydrazine decomposed gas. As the factor, the internal pressure in the plenum room decreases by the severe cathode erosion when using SHP163 decomposed gas. Therefore, it is necessary to take countermeasures against the severe cathode erosion in the future. Also, there is a possibility that gaseous water in SHP163 decomposed gas is cooled by water cooling of the anode part and returned to liquid. I think that the thrust performance may have deteriorated even by that. Therefore, we consider solving the problem by changing the anode part to the anode radiation cooling type instead of water cooling. In the future, keeping the temperature of the propellant high by radiant cooling for both electrodes is considered to lead to an improvement in performance with SHP163 decomposed gas.

7.2. Performance comparison with water-cooled arcjet thruster and prototype anode-radiation-cooled arcjet thruster

We confirmed stable operation with nitrogen using prototype anode-radiation-cooled arcjet thruster. As a result of the performance comparison, thrust performances of the prototype anode-radiation-cooled arcjet thruster is higher than that of the water-cooled arcjet thruster. This was because the thermal energy loss by water cooling at the anode was reduced.

7.3. Development of improved type anode-radiation-cooled arcjet thruster using thermal analysis

We developed improved type anode-radiation-cooled arcjet thruster for long time operation. Thermal analysis was conducted. All component temperature of the improved type anode-radiation-cooled arcjet thruster was acceptable.

7.4. Temperature comparison with analysis result and experimental result

Temperature measurement was conducted to verify the analysis result. The analysis result and experimental result had a good agreement temperature distribution. The maximum error was less than 20 K. In the future, we will use this thruster to acquire basic performance with nitrogen, acquire performance with SHP163 decomposed gas, and develop thrusters aiming to operate with low-toxicity propellants.

References

[1]Yuki Fukutome, Suguru Shiraki, Katsuya Shimogaito, Hirokazu Tahara, Kyoko Takada Yuichiro Nogawa an Ai Momozawa ”Performance and Thermal Characteristics of Low-Power Arcjet Thrusters for Water Propellant” The 2016 Asia-Pacific International Symposium on Aerospace Technology, Toyama, Japan, R1-3, 2016.

[2]Suguru Shiraki and Hirokazu Tahara “Performance and Thermal Characteristics of Low-Power DC Arcjet Thrusters with Radiation-Cooled Anodes for Green Propellants” AIAA Propulsion and Energy Forum and Exposition (Propulsion and Energy 2016), Salt Lake City, Utah, USA, AIAA-2016-4700, 2016.

[3]Yuki Fukutome, Suguru Shiraki, Fumihiro Inoue, Katsuya Shimogaito, Takashi Nakanishi, Hirokazu Tahara, Kyoko Takada, Yuichiro Nogawa and Ai Momozawa “Research and Development of Low-Power Arcjet thrusters with Green Propellants of HAN and Water” Space Propulsion 2016, Paper No. 3124903, 2016.

[4]Suguru Shiraki, Yuki Fukutome, Fumihiro Inoue, Katsuya Shimogaito, Takashi Nakanishi, Hirokazu Tahara and Kyoko Takada “Performance and Thermal Characteristics of Low-Power DC Arcjet Thrusters with Radiation-Cooled Anodes for Low-Toxicity Propellants” 8th Asian Joint Conference on Propulsion and Power (AJSPP 2016), Kagawa, Japan, AJCPP2016-116, 2016.

[5]Fumihiro Inoue, Yuki Fukitome, Suguru Shiraki, Kazuma Matsumoto, Hirokazu Tahara 「Performance and Thermal Characteristics of High-Power Hydrogen Arcjet Thrusters with Radiation-Cooled Anodes for In-Space Propulsion」 Joint Conf.: 30th International Symposium on Space Technology and Science (30th ISTS), 34th International Electric Propulsion Conference (34th IEPC), 6th Nano-Satellite Symposium (6th NSAT), Hyogo, Japan, IEPC-2015-231/ISTS-2015-b-231, 2015.